Research Article | Vol. 25, No. 18 | 4 Sep 2017 | OPTICS EXPRESS 21342
Optics EXPRESS

Second harmonic generation enhancement from a nonlinear nanocrystal integrated hyperbolic metamaterial cavity

WENYANG WU,[1] LINGLING FAN,[1] WENBO ZANG,[1] XIN YANG,[1] PENG ZHAN,[1,2,3] ZHUO CHEN,[1,2,*] AND ZHENLIN WANG [1,2,4]

[1]*School of Physics and National Laboratory of Solid State Microstructures, Nanjing University, Nanjing 210093, China*
[2]*Collaborative Innovation Center of Advanced Microstructures, Nanjing University, Nanjing 210093, China*
[3]*zhanpeng@nju.edu.cn*
[4]*zlwang@nju.edu.cn*
**zchen@nju.edu.cn*

Abstract: We theoretically investigate the dipolar whispering-gallery modes (WGMs) with different mode orders supported by spherical hyperbolic metamaterial (HMM) cavities consisting of alternating metal and dielectric layers. Associated with the excitations of the WGMs with the highest and the second highest mode orders, the HMM cavities are capable of creating highly enhanced and uniformly distributed local fields in the entire dielectric core region. Variation on the metal filling ratio allows for easily tuning the resonant wavelengths of WGMs over a wide spectral range. By integrating a nonlinear nanocrystal into the HMM cavities, we show enhancements of intensity of second harmonic generation up to a factor of 3.9×10^{10}, which is two orders of magnitude higher than the largest enhancement achieved in the single-layer plasmonic core-shell cavities.

OCIS codes: (250.5403) Plasmonics; (160.3918) Metamaterials; (190.2620) Harmonic generation and mixing.

References and links

1. J. A. Schuller, E. S. Barnard, W. Cai, Y. C. Jun, J. S. White, and M. L. Brongersma, "Plasmonics for extreme light concentration and manipulation," Nat. Mater. **9**(3), 193–204 (2010).
2. B. Luk'yanchuk, N. I. Zheludev, S. A. Maier, N. J. Halas, P. Nordlander, H. Giessen, and C. T. Chong, "The Fano resonance in plasmonic nanostructures and metamaterials," Nat. Mater. **9**(9), 707–715 (2010).
3. A. E. Schlather, N. Large, A. S. Urban, P. Nordlander, and N. J. Halas, "Near-Field Mediated Plexcitonic Coupling and Giant Rabi Splitting in Individual Metallic Dimers," Nano Lett. **13**(7), 3281–3286 (2013).
4. S. Kim, J. Jin, Y. J. Kim, I. Y. Park, Y. Kim, and S. W. Kim, "High-harmonic generation by resonant plasmon field enhancement," Nature **453**(7196), 757–760 (2008).
5. G. M. Akselrod, C. Argyropoulos, T. B. Hoang, C. Ciracì, C. Fang, J. Huang, D. R. Smith, and M. H. Mikkelsen, "Probing the mechanisms of large Purcell enhancement in plasmonic nanoantennas," Nat. Photonics **8**(11), 835–840 (2014).
6. E. M. Roller, C. Argyropoulos, A. Hogele, T. Liedl, and M. Pilo-Pais, "Plasmon-Exciton Coupling Using DNA Templates," Nano Lett. **16**(9), 5962–5966 (2016).
7. R. Chikkaraddy, B. de Nijs, F. Benz, S. J. Barrow, O. A. Scherman, E. Rosta, A. Demetriadou, P. Fox, O. Hess, and J. J. Baumberg, "Single-molecule strong coupling at room temperature in plasmonic nanocavities," Nature **535**(7610), 127–130 (2016).
8. A. Kinkhabwala, Z. Yu, S. Fan, Y. Avlasevich, K. Mullen, and W. E. Moerner, "Large single-molecule fluorescence enhancements produced by a bowtie nanoantenna," Nat. Photonics **3**(11), 654–657 (2009).
9. T. Siegfried, Y. Ekinci, O. J. F. Martin, and H. Sigg, "Gap Plasmons and Near-Field Enhancement in Closely Packed Sub-10 nm Gap Resonators," Nano Lett. **13**(11), 5449–5453 (2013).
10. J. Lee, J. Song, G. Y. Sung, and J. H. Shin, "Plasmonic Waveguide Ring Resonators with 4 nm Air Gap and λ_0^2/15,000 Mode-Area Fabricated Using Photolithography," Nano Lett. **14**(10), 5533–5538 (2014).
11. S. Panaro and C. Ciracì, "Nonlocal Plasmonic Response and Fano Resonances at Visible Frequencies in Sub-Nanometer Gap Coupling Regime," ACS Photonics **3**(12), 2467–2474 (2016).
12. M. Pellarin, J. Ramade, J. M. Rye, C. Bonnet, M. Broyer, M. A. Lebeault, J. Lermé, S. Marguet, J. R. G. Navarro, and E. Cottancin, "Fano Transparency in Rounded Nanocube Dimers Induced by Gap Plasmon Coupling," ACS Nano **10**(12), 11266–11279 (2016).

#302737 https://doi.org/10.1364/OE.25.021342
Journal © 2017 Received 19 Jul 2017; revised 20 Aug 2017; accepted 21 Aug 2017; published 23 Aug 2017
Corrected: 24 August 2017

Optics EXPRESS

13. H. Aouani, M. Rahmani, M. Navarro-Cía, and S. A. Maier, "Third-harmonic-upconversion enhancement from a single semiconductor nanoparticle coupled to a plasmonic antenna," Nat. Nanotechnol. **9**(4), 290–294 (2014).
14. A. Sundaramurthy, K. B. Crozier, G. S. Kino, D. P. Fromm, P. J. Schuck, and W. E. Moerner, "Field enhancement and gap-dependent resonance in a system of two opposing tip-to-tip Au nanotriangles," Phys. Rev. B **72**(16), 165409 (2005).
15. C. Ciraci, R. T. Hill, J. J. Mock, Y. Urzhumov, A. I. Fernández-Domínguez, S. A. Maier, J. B. Pendry, A. Chilkoti, and D. R. Smith, "Probing the Ultimate Limits of Plasmonic Enhancement," Science **337**(6098), 1072–1074 (2012).
16. Y. Pu, R. Grange, C. L. Hsieh, and D. Psaltis, "Nonlinear Optical Properties of Core-Shell Nanocavities for Enhanced Second-Harmonic Generation," Phys. Rev. Lett. **104**(20), 207402 (2010).
17. T. H. Park and P. Nordlander, "On the nature of the bonding and antibonding metallic film and nanoshell plasmons," Chem. Phys. Lett. **472**(4-6), 228–231 (2009).
18. C. F. Bohren and D. R. Huffman, *Absorption and Scattering of Light by Small Particles* (Wiley New York, 1983).
19. P. B. Johnson and R. W. Christy, "Optical constants of the noble metals," Phys. Rev. B **6**(12), 4370–4379 (1972).
20. C. Wu, A. Salandrino, X. Ni, and X. Zhang, "Electrodynamical light trapping using whispering-gallery resonances in hyperbolic cavities," Phys. Rev. X **4**(2), 021015 (2014).
21. M. Wan, P. Gu, W. Liu, Z. Chen, and Z. Wang, "Low threshold spaser based on deep-subwavelength spherical hyperbolic metamaterial cavities," Appl. Phys. Lett. **110**(3), 031103 (2017).
22. E. Prodan, C. Radloff, N. J. Halas, and P. Nordlander, "A hybridization model for the plasmon response of complex nanostructures," Science **302**(5644), 419–422 (2003).
23. R. W. Boyd, *Nonlinear Optics* (Academic Press: Burlington, MA, 2008).
24. P. Gu, M. Wan, Q. Shen, X. He, Z. Chen, P. Zhan, and Z. Wang, "Experimental observation of sharp cavity plasmon resonances in dielectric-metal coreshell resonators," Appl. Phys. Lett. **107**(14), 141908 (2015).
25. S. J. Oldenburg, S. L. Westcott, R. D. Averitt, and N. J. Halas, "Surface enhanced Raman scattering in the near infrared using metal nanoshell substrates," J. Chem. Phys. **111**(10), 4729–4735 (1999).
26. E. Iglesias-Silva, J. Rivas, L. M. León Isidro, and M. A. López-Quintela, "Synthesis of silver-coated magnetite nanoparticles," J. Non-Cryst, Sol. **353**, 829–831 (2007).
27. H. Chen, L. Shao, Y. C. Man, C. Zhao, J. Wang, and B. Yang, "Fano resonance in (Gold Core)-(Dielectric Shell) nanostructures without symmetry breaking," Small **8**(10), 1503–1509 (2012).
28. J. F. Li, Y. F. Huang, Y. Ding, Z. L. Yang, S. B. Li, X. S. Zhou, F. R. Fan, W. Zhang, Z. Y. Zhou, D. Y. Wu, B. Ren, Z. L. Wang, and Z. Q. Tian, "Shell-isolated nanoparticle-enhanced Raman spectroscopy," Nature **464**(7287), 392–395 (2010).

1. Introduction

Localized surface plasmon resonances (LSPRs) supported by metallic nanostructures have the ability to concentrate light into subwavelength volumes and give rise to strongly enhanced electromagnetic fields [1], which enables their use in a wide range of nanophotonics technologies and devices [2]. In the past few years, great efforts have been made to further increase the maximum field enhancement by rationally designing the plasmonic nanostructures. For example, as compared to the single metal nanoparticles, dimers and nanoparticle-on-mirror nanopatch structures could produce a more intense local field with amplitude enhancement factor up to 10^2-10^3 [3–5]. Since these coupled plasmonic nanostructures are based on the strong coupling between two nanoparticles in the dimers or between nanoparticle and its image in the nanopatches, nanometer or sub-nanometer gaps are required, which is perfectly suitable for enhance the light-matter interactions at nanometer scale [4–12]. For example, by exploiting high field enhancements and embedding gas or dye molecules within the nanogaps, high-harmonic generation [4], large fluorescence and Purcell enhancement [5,8], and even single-molecule strong coupling have been experimentally demonstrated [7]. Although plasmonic dimers have recently been employed to enhance the third harmonic generation from the 25-nm-diameter indium tin oxide nanoparticles located at the dimer gaps [13], the gap width has to be widened to several tens of nanometers to accommodate the relative large nonlinear nanoparticles, which could dramatically weaken the field enhancement due to the weaker coupling between paired plasmonic nanoparticles with increasing gaps [14,15]. By coating the nonlinear nanoparticles with a thin gold shell to form plasmonic core-shell nanocavities, it has been demonstrated that the efficiency of second harmonic generation (SHG) could also be enhanced as a result of the full-utilization

Optics EXPRESS

of the mode volume of the cavity [16]. However, for a gold nanoshell the field enhancement in the core region is typically limited to the order of 10 [17].

In this paper, we demonstrate that spherical hyperbolic metamaterial (HMM) cavities, consisting of a dielectric nano-core wrapped by several alternating layers of metal and dielectric, could support a set of dipolar whispering-gallery modes (WGMs). Associated with the excitations of the dipolar WGMs with the highest and the second highest mode orders, the electric fields are found to be enhanced strongly and distributed uniformly within the entire core region. Furthermore, by varying the ratio of the metal shell thickness to the multilayer period, the dipolar resonances could be tuned over a wide spectral range. Such desirable characteristics make the HMM cavities integrated with a nonlinear nanocrystal core suitable for application in nanoscale efficient coherent nonlinear optical light sources. By integrating a 10-nm-radius nanocrystal into a 4-pair HMM cavity, we show enhancements of SHG intensity at a fundamental wavelength of 810 nm up to a factor of 3.9×10^{10}, which is two orders of magnitude higher than the achievable maximum enhancement in the single-layer plasmonic core-shell case.

2. Results and discussions

Figure 1(a) shows the schematic of a spherical HMM cavity, consisting of a nonlinear dielectric core (radius: r) alternately wrapped by metal (thickness: t) and dielectric (thickness: d) layers. Throughout this paper, the refractive indice of the dielectric core and shell are assumed to be n = 2.5 (e.g. $BaTiO_3$) and n = 1.5 (e.g. SiO_2), respectively. The problem of extinction of a plane wave by the HMM cavities embedded in the air is solved analytically using Mie theory [18]. Figure 1(b) shows the extinction efficiency spectra of the HMM cavities with the same dielectric core radius of r = 10 nm but a different number (N) of functional pairs (each pair is consisting of one dielectric layer and one metal shell layer). In the calculations, only the dipolar term (a_1) of Mie expansion is taken into account, since the cavity is much smaller than the wavelength. The metal is assumed to be silver and its dielectric constant (ε_m) is taken from the experimental data of Johnson and Christy [19]. For simplicity, the thickness of the dielectric shell is set to be equal to the core radius ($d = r$ = 10 nm). The filling ratio of the metal shell thickness to the multilayer period $f = t/(t+d)$ is fixed to be f = 0.1. Under the effective medium description, the permittivity tensor of the metamaterial shell in our case takes the form of $\varepsilon_{eff} = \hat{r}\hat{r}\varepsilon_r + \hat{\theta}\hat{\theta}\varepsilon_t + \hat{\phi}\hat{\phi}\varepsilon_t$, where we consider $\varepsilon_r = \varepsilon_m n^2 / [\varepsilon_m (1-f) + n^2 f] > 0$ and $\varepsilon_t = \varepsilon_m f + n^2 (1-f) < 0$ [20]. It has been demonstrated that spherical HMM cavities could support multipolar WGMs, which are caused by the indefinite nature of the permittivity tensors. Due to the Mie-mode nature, WGMs with the same angular momentum (l) could have different mode orders [18]. Lower mode order corresponds to a longer resonance wavelength and the maximum field enhancement localized within the more external dielectric shell layer [21]. It is seen from Fig. 1(b) that extinction peaks appear in the spectra as a result of the excitations of the dipolar WGMs with different mode orders. Noting that each mode in the spectrum has the same angular momentum l = 1, and thus is identified by WGM_m, where m denotes the mode order (radial mode number, $1 \le m \le N$). By increasing the number of functional pairs, the resonances with the same mode order undergo a redshift [Fig. 1(b)], as expected, since the multilayer cavity can be better described as an effective medium [20,21]. The resonances with the highest mode order (WGM_N resonances) are found to blue-shift from λ = 878 nm to λ = 817 nm with increasing the number of the functional pairs from N = 1 to N = 3 [Fig. 1(b)]. In particular, as the number of functional pairs increases beyond N = 3, the blue-shift of the WGM_N resonances tends to converge to a wavelength of ~810 nm.

Optics EXPRESS

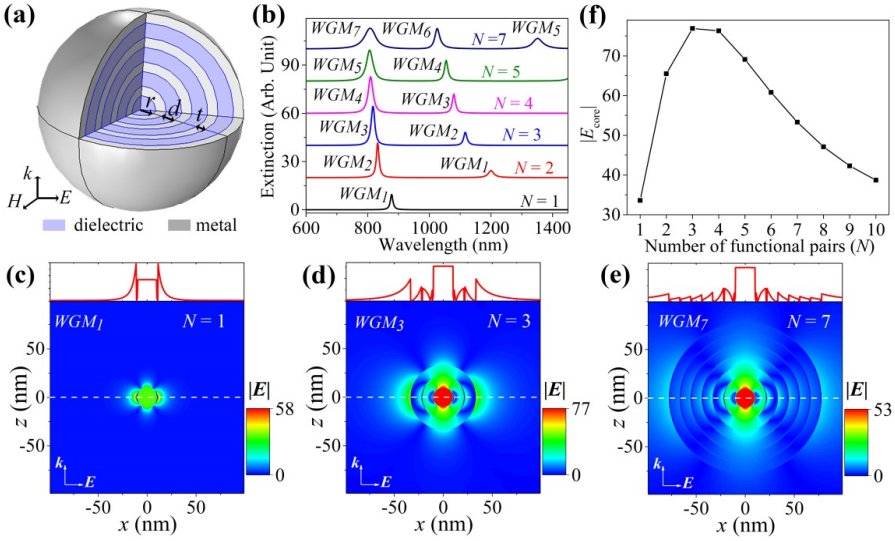

Fig. 1. (a) Schematic of a spherical HMM cavity with 4 functional pairs. The refractive index of the dielectric core is $n = 2.5$ and its radius is r. Each pair is constituted of a dielectric layer (refractive index: $n = 1.5$, thickness: d) and a silver shell layer (thickness: t). (b) Extinction efficiency spectra of the HMM cavities with different numbers of functional pairs. The core radius and the dielectric shell thickness are assumed to be $r = d = 10$ nm. The metal filling ratio is fixed to be $f = 0.1$. For clarity, each curve is shifted vertically by a constant relative to the previous one. (c)-(e) Electric field amplitude enhancement distributions of the resonances WGM_1, WGM_3, and WGM_7 in 1-pair, 3-pair, and 7-pair HMM cavities, respectively. The upper panels present the field amplitude along the cross sections indicated by dashed lines in the lower panels. (f) Summarization of the amplitude enhancement of the electric field taken at a point 0.1 nm away from the center of the HMM cavities with different numbers of functional pairs.

Figures 1(c)-1(e) show the spatial distributions of the electric field amplitude enhancement ($|E/E_0|$) calculated at the resonances WGM_1, WGM_3 and WGM_7 supported by 1-pair, 3-pair, and 7-pair HMM cavities, respectively. In all cases, the electric fields inside the dielectric core are found to have only one component, which is parallel to the direction of polarization of the incident electric field. The electric fields are also found to be distributed uniformly within the entire core region, which could be more clearly seen from the upper panels of Figs. 1(c)-1(e) where we analyze the electric field along the white dashed lines in the corresponding spatial distributions. For $N = 1$, the HMM cavity is a single-layer metal nanoshell, and the WGM_1 resonance is actually a bonding mode [22]. Although the maximum field enhancements are located on the outer surface of the nanoshell, the field enhancement inside the dielectric core could reach a value of ~33 [Fig. 1(c)], which is a reason that the plasmonic core-shell has been employed to enhance the SHG efficiency from a nanocrystal [16]. With increasing the number of functional pairs to $N = 3$, the HMM cavity is able to more tightly confine the electric fields within the dielectric core, and thus produce a higher field enhancement factor of ~77 associated with the excitation of the WGM_3 resonance [Fig. 1(d)], which is about 2.3 times larger than that in the 1-pair HMM cavity [Fig. 1(c)]. However, further increase in the number of functional pairs could lead to a drop in the field enhancement obtained inside the dielectric core, which is mainly due to the decreased excitation efficiency of the WGMN resonances resulting from the increased total thickness of the metal shells [Fig. 1(b)]. For example, as the number of functional pairs is increased to $N = 7$, the field enhancement inside the dielectric core is found to decrease to a value of ~53 [Fig. 1(e)]. These findings are further supported by Fig. 1(f) where we summarize the amplitude enhancement of the electric field monitored at a point 0.1 nm away

Optics EXPRESS

from the center of the HMM cavities, which clearly presents a trend of first increase and then decrease in the field enhancement with increasing the number of functional pairs.

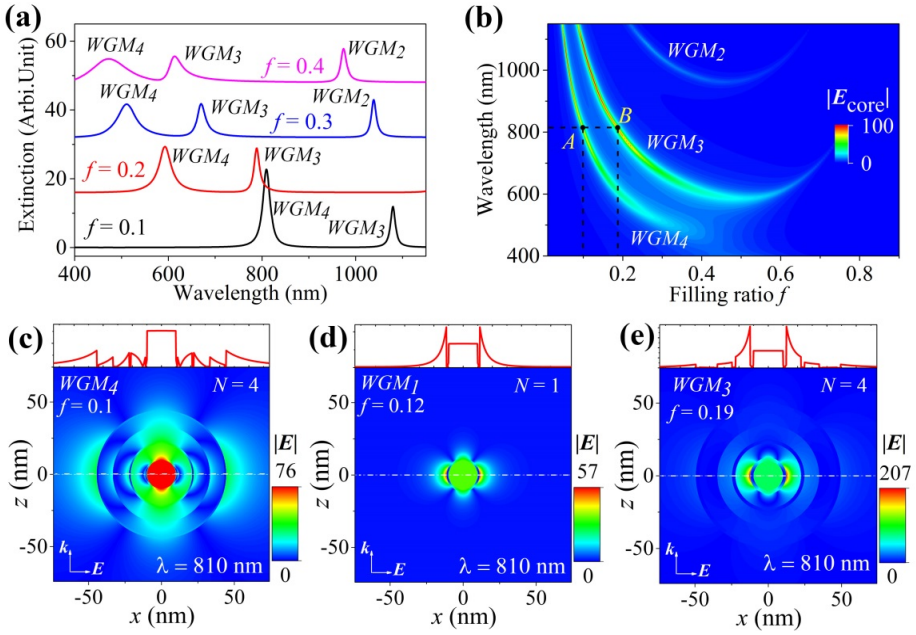

Fig. 2. (a) The extinction spectra of 4-pair HMM cavities with four different metal filling ratios. The core radius and dielectric shell thickness are fixed to be $r = d = 10$ nm. Each curve is shifted vertically by a constant relative to the previous one. (b) Amplitude enhancement of the electric field taken at a point 0.1 nm away from the center as functions of the metal filling ratio and wavelength. Marked points A and B indicate the particular filling ratios of $f = 0.1$ and 0.19 where the WGM_4 and WGM_3 resonances can produce the maximum field enhancement at the wavelength of 810 nm, respectively. (c) Field distribution of the WGM_4 resonance supported by a 4-pair HMM cavity with filling ratio corresponding to the marked point *A* in (b). (d) Field distribution of the WGM_1 supported by a 1-pair HMM cavity with core radius of $r = 10$ nm and filling ratio of $f = 0.12$. (e) Similar to (c) but for the WGM_3 resonance and filling ratio corresponding to the marked point *B* in (b). The upper panels in (c)-(e) present the field amplitude along the cross sections indicated by dashed lines in the lower panels.

It has already been demonstrated that in the single-layer metal nanoshell structures, the resonance wavelengths are dependent on the relative dimensions of the dielectric core and metal shell [22]. Similarly, the spectral positions of the resonances in the multilayer HMM cavity could be tuned by varying the metal filling ratio (*f*) [20,21]. Figure 2(a) shows the extinction efficiency spectra of 4-pair HMM cavities with different filling ratios, where the parameters of the dielectric core ($n = 2.5$, $r = 10$ nm) and dielectric shell ($n = 1.5$, $d = 10$ nm) are the same as those used in Fig. 1(b). In this case, the filling ratio $f = t/(t+d)$ could be varied by solely changing the thickness of the metal shell *t*. It is clearly seen from Fig. 2(a) that all the resonances can be tuned to the longer wavelengths with decreasing the filling ratio *f*. The amplitude enhancement of the electric field monitored at a point 0.1 nm away from the center of the HMM cavities is plotted in Fig. 2(b) as functions of the metal filling ratio and the wavelength. It is seen from Fig. 2(b) that the field enhancement associated with the excitation of each resonance follows the same trend of resonance red-shifting with decreasing the filling ratio *f*. As marked by the point *A* in Fig. 2(b), associated with the excitation of the resonance with the highest mode order (WGM_4), the 4-pair HMM cavity with a filling ratio of $f = 0.1$ can produce the maximum field enhancement at $\lambda = 810\,\text{nm}$, which is close to the output wavelength of a Ti:sapphire oscillator. Figure 2(c) shows the

Optics EXPRESS

field distribution of WGM_4 supported by the HMM cavity with $f = 0.1$ corresponding to the marked point A in Fig. 2(b). The electric field is again found to be distributed uniformly within the entire core region, and its enhancement can reach a factor of 76. For comparison, the field distribution of the WGM_1 resonance supported by a 1-pair HMM cavity is shown in Fig. 2(d), where the dielectric core has the same radius ($r = 10$ nm) and refractive index ($n = 2.5$) as that for 4-pair HMM cavity, and the metal filling ratio is set to $f = 0.12$ such that the WGM_1 resonance is resonant at $\lambda = 810$ nm. In this case, the field enhancement inside the dielectric core could only reach a value of ~33, which is much smaller than that in the 4-pair HMM cavity [Fig. 2(c)].

Moreover, it is seen from Figs. 2(a) and 2(b) that the resonance with the second highest mode order (WGM_3 for $N = 4$) also exhibits spectral tunability and produces a relatively large field enhancement inside the cavity. As compared to the resonance WGM_4, a larger filling ratio is required to tune the resonance WGM_3 to a given wavelength, since the resonance with a lower mode order corresponds to a longer resonance wavelength. The larger filling ratio leads to a thicker metal shell layer, which avoids the necessity for ultrathin metal film, making the multilayer HMM cavity more easily constructed. As marked by the point *B* in Fig. 2(b), when the filling ratio is taken to a relatively large value of $f = 0.19$ the resonance WGM_3 can produce the maximum field enhancement at $\lambda = 810\,\text{nm}$. The spatial distribution of the field amplitude enhancement of the WGM_3 resonance supported by a 4-pair HMM cavity with a filling ratio of $f = 0.19$ [corresponding to the marked point *B* in (b)] is shown in Fig. 2(e). As expected, the maximum field enhancements associated with the excitation of the WGM_3 resonance locate on the third dielectric shell layer, counting inward toward the center. Interestingly, it is seen from either the bottom or top panel of Fig. 2(e) that the field enhancement in the neighboring dielectric shell layer could induce uniformly distributed electric fields inside the dielectric core. In particular, the field amplitude enhancement within the dielectric core could reach a value of 85 [Fig. 2(e)], which is even higher than that achieved in the WGM4 resonance [Fig. 2(c)].

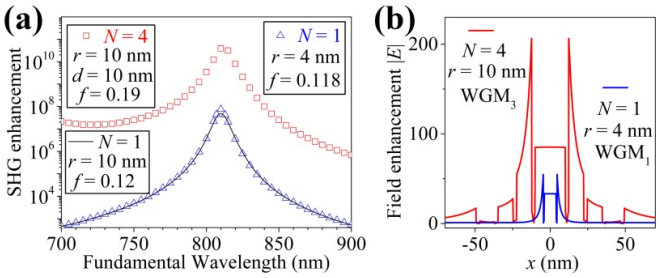

Fig. 3. (a) The SHG enhancement calculated for a 4-pair HMM cavity with $r = d = 10$ nm and $f = 0.19$ (red open squares), a 1-pair HMM cavity with $r = 4$ nm and $f = 0.118$ (blue open triangles), and a 1-pair HMM cavity with $r = 10$ nm and $f = 0.12$ (black solid line). (b) Electric field amplitude enhancement along a cross-section-line at $z = 0$ nm for the WGM_3 resonance supported by the 4-pair HMM cavity with $r = d = 10$ nm and $f = 0.19$ (red curve) and the WGM_1 resonance supported by the 1-pair HMM cavity with $r = 4$ nm and $f = 0.118$ (blue curve).

In the following, we demonstrate that the multilayer HMM cavities could generate SHG more efficiently than single-layer plasmonic core-shell structures. Figure 3(a) shows example calculations of the SHG enhancement (compared to the bare core) for 1-pair and 4-pair HMM cavities integrated with a $BaTiO_3$ nanocrystal, which are conducted using the three-dimensional finite-element-method (FEM) software COMSOL Multiphysics. In the first calculation step, instead of using Mie theory, the electric fields $\mathbf{E}_\omega$ at the fundamental wavelength (fundamental frequency ω) are re-calculated in FEM software. In the second step, the numerically obtained fundamental electric fields inside the core are directly used in

Optics EXPRESS

FEM software to construct the second-order nonlinear polarization of the HMM cavity $P_{2\omega} = \varepsilon_0 d \cdot E_\omega E_\omega$ and compute the nonlinear response at the second-harmonic wavelength (second-harmonic frequency 2ω), where **d** is the second-order nonlinear optical coefficient tensor of $BaTiO_3$. As have been demonstrated above, the electric field inside the dielectric core at the WGM resonances has only one component with its direction parallel to the polarization of the incident light. Therefore, by choosing an appropriate angle between the polarization of the incident light and the *c*-axis of the $BaTiO_3$ nanocrystal, the second-order susceptibility of $BaTiO_3$ nanocrystal can be approximated as an isotropic value of 15.7 pm/V (corresponding to d_{31} coefficient) [23]. As have been demonstrated above, for a 4-pair HMM cavity with a core radius of r = 10 nm, a dielectric shell thickness of d = 10 nm, and a filling ratio of f = 0.19 [corresponding to the marked point *B* in (b)], the dipolar resonance with the second highest mode order (WGM_3) is resonant at 810 nm. In order to tune the WGM_1 resonance supported by the 1-pair HMM cavity (single-layer core-shell structure) to the same wavelength of 810 nm, the core radius and the filling ratio are taken to be r = 4 nm and f = 0.118, respectively. It is seen from Fig. 3(a) that when the 1-pair and 4-pair HMM cavities are pumped at 810 nm, the factor of SHG enhancement in the 4-pair HMM cavity could reach a high value of 3.899×10^{10} (open squares), which is two orders of magnitude higher than the enhancement factor of 7.573×10^7 achieved in the 1-pair HMM cavity (open triangles). Figure 3(b) shows the field amplitude enhancement extracted along a central cross-section-line (z = 0 nm) for the WGM_3 resonance supported by a 4-pair HMM cavity with $r = d$ = 10 nm and f = 0.19 (red curve) and the WGM_1 resonance supported by the 1-pair HMM cavity with r = 4 nm and f = 0.118 (blue curve), which directly confirms that the field enhancement in the 4-pair HMM cavity is much higher than that in the 1-pair HMM cavity. It should be noted that r = 4 nm and f = 0.118 are the optimal parameters for a single-layer core-shell structure to achieve the maximum SHG enhancement at 810 nm. Figure 3(a) also shows the SHG enhancement for an additional 1-pair HMM cavity with r = 10 nm and f = 0.12, which has the same core size as the 4-pair HMM cavity and is also resonant at 810 nm. In this case, the obtained SHG enhancement factor of 7.285×10^7 at 810 nm [solid line in Fig. 3(a)] is indeed smaller than that in the optimal case [open triangles in Fig. 3(a)].

3. Conclusions

In conclusion, we demonstrate that spherical HMM cavities composed of N ($N > 1$) pairs of alternating metal and dielectric layers could support a set of dipolar WGM resonances with the mode order ranging from m = 1 to $m = N$. As compared to the single-layer plasmonic core-shell cavity (N = 1), the multilayer HMM cavities exhibit higher field enhancements inside the dielectric core arising from the excitations of the WGM resonances with the highest more order (WGM_N) and the second highest mode order (WGM_{N-1}). In both cases, the electric fields are distributed uniformly within the entire core region, and have only one component with its direction parallel to the polarization of the incident light. In addition, the spectral positions of the WGM resonances could be easily tuned over a wide range by varying the metal filling ratio in the HMM cavities. We suggest that the spherical HMM cavities can be prepared by using physical deposition process [24] or wet-chemistry method [25–28] to surround a dielectric core with alternating metal and dielectric shell layers. Although only SHG enhancement has been theoretically demonstrated in the 4-pair HMM cavities integrated with a nonlinear core, the resonance tunability coupled with the ability to produce highly enhanced and uniformly distributed local fields inside the core make the HMM cavities also suitable for improving the efficiency of other nonlinear processes.

Funding

National Key R&D Program of China (Grant No. 2017YFA0303700), National Nature Science Foundation of China (NSFC) (11674168, 11474215 and 11621091).